

## CHAPTER 4

### RESULTS AND DISCUSSION

#### 4.1 Fungal cultivation, laccase activity and dye decolorization assay

Figure 4.1 showed the morphology of *P. sanguineus* pellets in the GYMP medium. After four (4) days of cultivation on rotary shaker, the fungus formed puffy balls consisting of a dense mycelial network with the average size of pellets at  $2.6 \pm 0.5$  mm. Hairy appearance was observed on the surface of pellets.

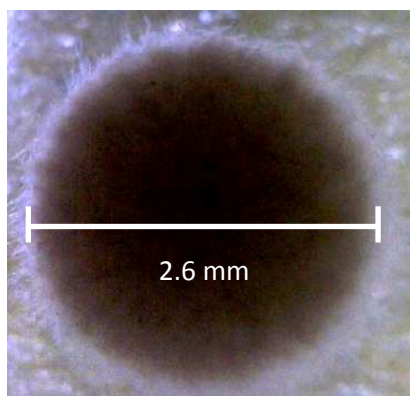


Figure 4.1: Morphological pellets

Laccase activity assay showed that there was no soluble laccase produced by fungus in the shake flask during four (4) days cultivation period in the GYMP rich medium. According to Buswell *et al.* (1984), lignin modifying enzymes (LME) production occurs during secondary metabolism induced by limited nutrient levels, particularly nitrogen. In this study, significant laccase activities inside the dye filtrate following decolorization by the fungus have been detected at approximately  $0.01 \pm 0.0003 \text{ U mL}^{-1}$ . It was hypothesized that upon exposure of the fungal biomass to the dye

solution which contained extremely low nutrient's levels, laccase production was elicited.

Spectral analysis of the crystal violet dye was initially done prior to dye decolorization analysis. Figure 4.2 showed that crystal violet strongly absorbed the light at 590 nm. Decolorization was followed by the disappearance of the dye in the aqueous solution. This disappearance was monitored via decreases in the solution's absorbance at the wavelength of 590 nm. Figure 4.3 showed standard calibration of absorbance at 590 nm against different concentrations of crystal violet, where the dye concentration ranged from 0 ppm to 5 ppm. This calibration was used to calculate the residual crystal violet concentration in the aqueous solution after decolorization process. The standard calibration fitted the equation (7):

$$C_{dye} = 0.191A_{590} \quad (7)$$

where  $C_{dye}$  is the concentration of the dye in ppm and  $A_{590}$  is the absorbance of the dye solution at 590 nm. Equation (4) had a regression coefficient of 0.998.

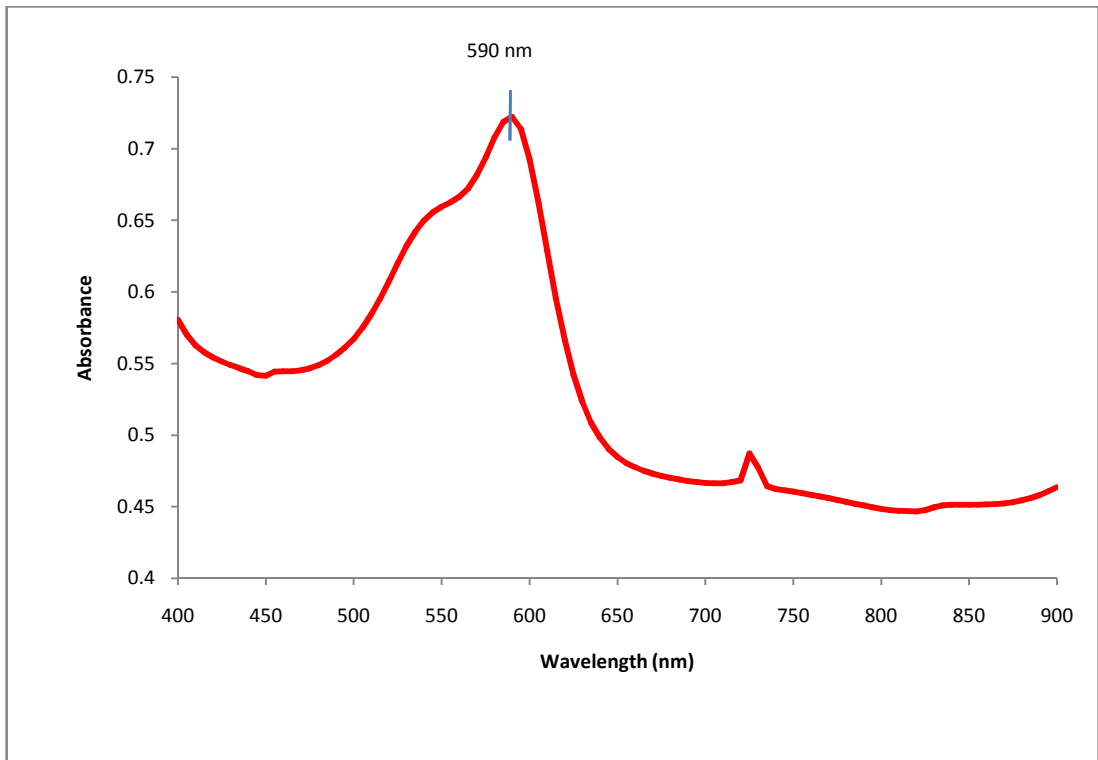


Figure 4.2 : UV-Vis absorption spectra of crystal violet

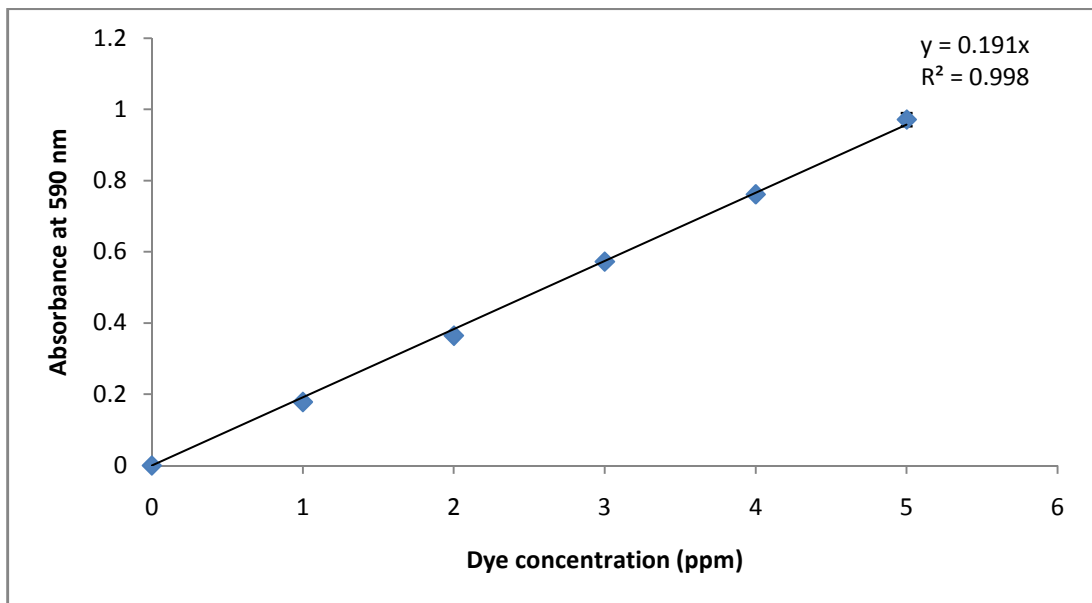


Figure 4.3: Standard curve for crystal violet dye

Figure 4.4 showed that the treated dye sample was nearly colourless and did not absorb light significantly particularly at 590 nm and generally in the visible region. This indicated that colour removal was practically complete or nearly complete. The

disappearance of the absorption signal at 590 nm reflected an almost complete decolorization of crystal violet.

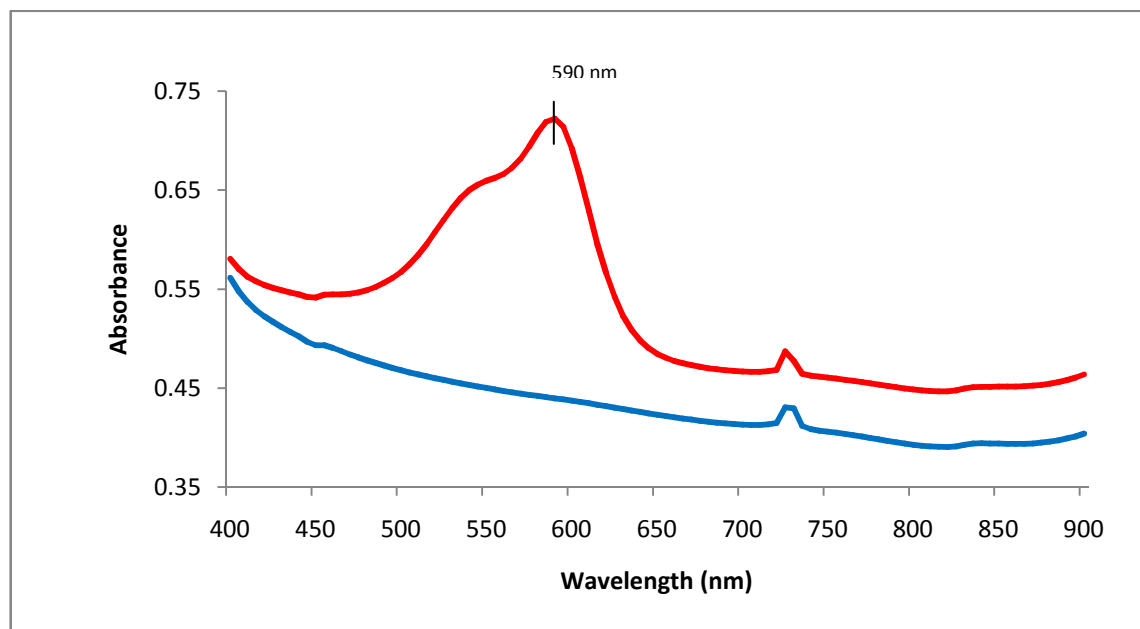


Figure 4.4: UV-Vis absorption spectra of crystal violet before (—) and after (—) decolorization

## 4.2 Optimization of dye decolorization process

Optimization experiment was developed using response surface experimental design (Table 4.1). There are three variables investigated *viz.* process time, agitation speed and initial dye concentration. The experimental data values of the studied variables are tabulated in Table 4.2.

Table 4.1: Box-Behnken response surface design for dye decolorization of crystal violet by *Pycnoporus sanguineus*: process time, agitation speed and initial dye concentration in coded unit along with the experimental and predicted response of percentage of decolorization (%).

Run	X1	X2	X3	Percentage of Decolorization (%)	
				Experimental	Predicted
1	-1	-1	0	68.48	70.27
2	0	0	0	93.73	93.53
3	0	0	0	88.59	91
4	1	0	1	86.67	86.06
5	0	1	1	95.42	91.41
6	1	1	0	90.06	86.02
7	-1	0	-1	86.72	85.31
8	0	0	0	94.41	93.53
9	0	0	0	93.93	93.53
10	1	0	-1	90.78	91
11	0	-1	-1	77.08	81.36
12	0	1	-1	81.28	91.41
13	1	1	0	88.31	86.02
14	-1	-1	0	68.47	70.27
15	1	0	1	88.93	91
16	1	1	0	89.32	86.02
17	-1	1	0	86.48	86.06
18	-1	0	1	86.58	85.31
19	0	-1	1	86.44	81.36
20	0	0	0	94.5	93.53
21	-1	0	1	85.54	85.31
22	0	1	1	95.38	91.4
23	0	-1	1	86.67	81.36
24	0	1	-1	86	91.41
25	0	-1	1	87.93	81.36
26	-1	1	0	88.36	86.06
27	1	-1	0	82.52	81.69
28	0	-1	-1	78.8	81.36
29	-1	-1	0	67.4	70.27
30	0	1	-1	82.14	91.41
31	1	-1	0	81.07	81.7
32	1	-1	0	81.32	81.7
33	0	0	0	94.21	93.53
34	-1	0	-1	84.88	85.31
35	0	0	0	94.13	93.53
36	1	0	-1	90.24	91
37	0	0	0	93.71	93.53
38	-1	0	1	85.94	85.31
39	0	0	0	94.64	93.53

40	1	0	-1	90.06	91
41	0	1	1	95.28	91.41
42	1	0	1	87.93	91
43	-1	0	-1	85.36	85.31
44	0	0	0	94.88	93.53
45	0	-1	-1	77.86	81.36

$X1$  = process time (day)  $X2$  = agitation speed (rpm)  $X3$  initial dye concentration (ppm)

Table 4.2: Coded levels and their actual values for process time, agitation speed and initial dye concentration variables.

Coded level	Process time (day)	Agitation speed (rpm)	Initial dye concentration (ppm)
1	1	60	5
0	2	110	22.5
-1	3	160	40

A full quadratic was initially fitted to the experiment data and results in the following expression:

$$y = 3.6952 + 31.7217 X1 + 0.8319 X2 + 0.2758 X3 - 5.4635 X1^2 - 0.0029 X2^2 - 0.0037 X3^2 - 0.0573 X1X2 - 0.0320 X1X3 + 0.0009 X2X3 \quad (8)$$

where is  $X1$  = process time (day),  $X2$  = agitation speed (rpm) and  $X3$  = initial dye concentration (ppm)

According to the estimated regression coefficient result (Table 4.3), about 86% of the variability in the dye decolorization data could be explained by the model. The adjusted R-square was calculated at 82.3 % indicating that the current model was satisfactory in modeling the data with respect to other models. Montgomery (2001) stated that the values of “Prob > F” less than 0.05 indicate the model terms to be significant while values greater than 0.1 indicate that model terms are not significant. It is shown that process time, agitation speed, combination of process time, square effect of agitation speed and interaction effect between process time and agitation speed have

significant effect on the decolorization process of crystal violet by *P. sanguineus* ( $P < 0.05$ ).

However, initial dye concentration and any other variables that have interactions with initial dye concentration were insignificant towards the decolorization process in terms of their effect. Analysis of variance (ANOVA) of the data was summarized in Table 4.4.

Process time is considered a significant factor influenced the decolorization process based on the followings:

- a) it is hypothesized that longer exposure to the dye solution will increase the percentage of its decolorization by fungal enzyme(s), as a result of increased probability of successful enzyme-dye interactions which resulted in decolorization. However, prolonged exposure to the crystal violet solution could inhibit or kill the fungus as this dye has been used as an agent to control fungal growth (Zolinger, 1987);
- b) since solid fungal pellets with defined sizes and spherical shape were used, diffusion time of the dye from bulk solution to the reaction sites, on the surfaces and within the pellets needs to be taken into consideration.

Agitation speed is also the significant factor that was influenced the decolorization process of *P. sanguineus*. The higher agitation speed will maintain the catalyst in the suspension condition and introduce the shear stress to the system. This will influence the catalyst behavior in the process. Shear stress may be influence the production of laccase into the system. However, increased the shear stress due to the increase in agitation intensity may damage the catalysts.

Table 4.3: Estimated regression coefficients for percentage of decolorization (%) model.

Term	Coef	SE Coef	T	P
Constant	3.6952	7.60245	0.486	0.630
Process time (days)	31.7217	4.24850	7.467	0.000
Agitation speed (rpm)	0.8319	0.08973	9.271	0.000
Initial dye concentration (ppm)	0.2758	0.19996	1.379	0.177
Process time (days) * Process time (days)	-5.4635	0.89656	-6.094	0.000
Agitation speed (rpm) * Agitation speed (rpm)	-0.0029	0.00036	-8.071	0.000
Initial dye concentration (ppm) * Initial dye concentration (ppm)	-0.0037	0.00293	-1.277	0.210
Process time (days) * Agitation speed (rpm)	-0.0573	0.01723	-3.326	0.002
Process time (days) * Initial dye concentration (ppm)	-0.0320	0.04922	-0.651	0.519
Agitation speed (rpm) * Initial dye concentration. (ppm)	0.0009	0.00098	0.906	0.371

S = 2.984 R<sup>2</sup> = 85.9% R<sup>2</sup> (adj) = 82.3 %

Note. SE, standard Error; T, T-statistic; P, P-statistic; S, error term; R<sup>2</sup>, coefficient of determination; R<sup>2</sup> (adj), adjusted coefficient of determination

Table 4.4: Analysis of variance for percentage of decolorization (%)

Source	DF	Seq SS	Adj SS	Adj MS	F	P
Regression	9	1906.35	1906.35	211.816	23.79	0.000
Linear	3	947.87	1043.63	347.878	39.07	0.000
Square	3	848.90	848.90	282.968	31.78	0.000
Interaction	3	109.57	109.57	36.525	4.10	0.014
Residual Error	35	311.63	311.63	8.904		
Lack-of-Fit	3	286.07	286.07	95.356	119.36	0.000
Pure Error	32	25.56	25.56	0.799		
Total	44	2217.98				

Note. DF, Degree of freedom; seq SS, sequential sum of squares; Adj SS, Adjusted sum of squares; Adj MS, Adjusted mean of squares



Since initial dye concentration and its respective interaction with process time and agitation speed were found to be statistically insignificant, an attempt was made to further reduce the regression model. Table 4.5 showed the estimated reduced regression model coefficients for percentage of decolorization excluding dye concentration factor and any other interactions with this factor. The resulting output indicated that the agitation speed and process time as a main factor have significant effect on decolorization process of crystal violet. The equation for this reduced model is:

$$y = 8.0818 + 30.6483X1 + 0.8442X2 - 5.3754X1^2 - 0.0029X2^2 - 0.0573X1X2 \quad (9)$$

where is  $X1$  = process time (day) and  $X2$  = agitation speed (rpm). The ANOVA of the data was summarized in Table 4.6.

Table 4.5: Estimated regression coefficients for percentage of decolorization (%) for process time, agitation speed, square effect for both process time and agitation speed, and interaction between process time and agitation speed

Term	Coef	SE Coef	T	P
Constant	8.0818	7.83174	1.032	0.308
Process time (days)	30.6483	4.83338	6.341	0.000
Agitation speed (rpm)	0.8442	0.10244	8.240	0.000
Process time (days) * Process time (days)	-5.3754	1.05577	-5.091	0.000
Agitation speed (rpm) * Agitation speed (rpm)	-0.0029	0.00042	-6.770	0.000
Process time (days) * Agitation speed (rpm)	-0.0573	0.02035	-2.816	0.008

S = 3.524 R-Sq = 78.2% R-Sq(adj) = 75.4%

Note. SE, standard Error; T, T-statistic; P, P-statistic; S, error term;  $R^2$ , coefficient of determination;  $R^2$  (adj), adjusted coefficient of determination

Table 4.6: Analysis of variance for percentage of decolorization (%) for process time, agitation speed, square effect for both process time and agitation speed, and interaction between process time and agitation speed

Source	DF	Seq SS	Adj SS	Adj MS	F	P
Regression	5	1733.58	1733.58	346.72	27.91	0.000
Linear	2	800.70	1093.82	546.91	44.03	0.000
Square	2	834.38	834.38	417.19	33.59	0.000
Interaction	1	98.50	98.50	98.50	7.93	0.008
Residual	39	484.40	484.40	12.42		
Error						
Lack-of-Fit	3	105.14	105.14	35.05	3.33	0.030
Pure Error	36	379.26	379.26	10.53		
Total	44	2217.98				

Note. DF, Degree of freedom; seq SS, sequential sum of squares; Adj SS, Adjusted sum of squares; Adj MS, Adjusted mean of squares

### 4.3 Analysis of normality assumption for the experimental data and model prediction data

The normality of the experimental data was checked using the normal probability plot (Figure 4.5). The data points were distributed reasonably close to the normality line except for several data points at both tail ends of the distribution. Based on this observation, there is no reason to suspect a huge deviation from normal assumption for the experimental data.

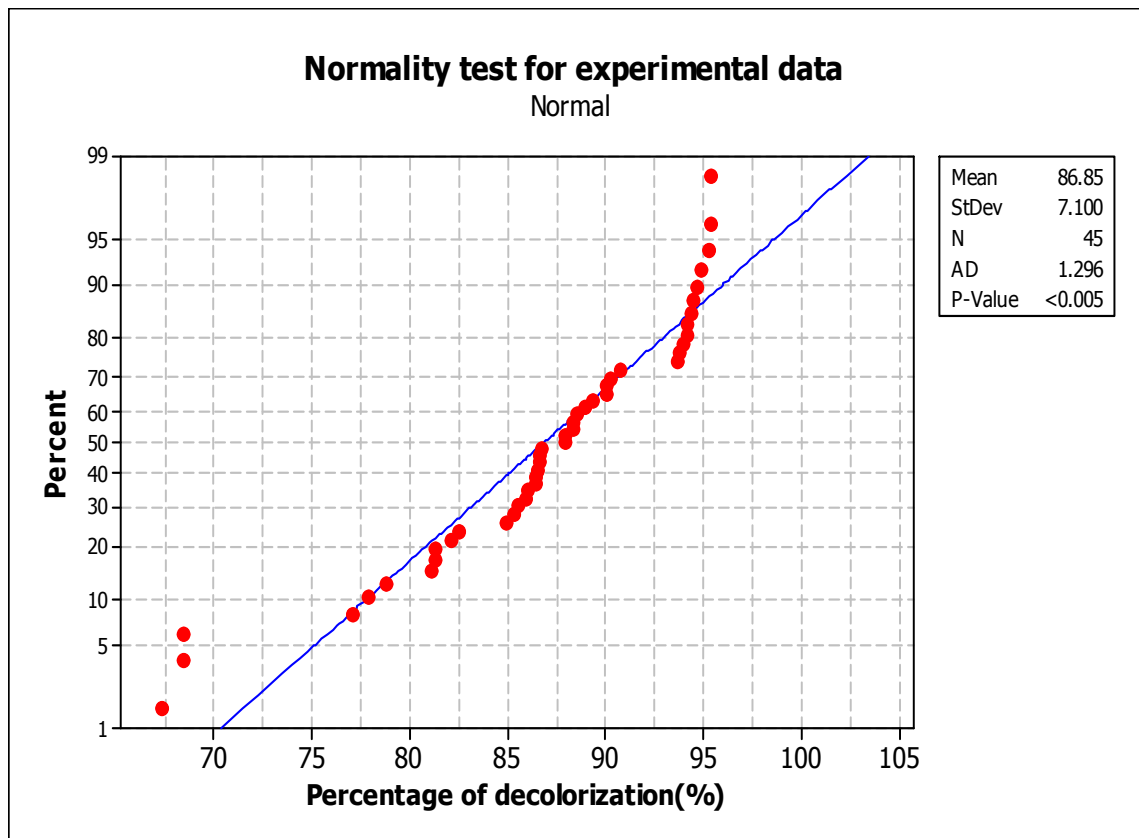


Figure 4.5: Normality test for experimental data

Figure 4.6 showed residuals (residual = experimental value - model predicted value) plots for percentage of decolorization of crystal violet by *P. sanguineus*. In the analysis of variance, it is usually more effective to construct the normal probability plot with the residuals. The normal probability plot of residuals (Figure 4.6A) showed normal distribution as this plot resemble a straight line, where more emphasis is placed on the central values of the plot than on the extremes. Thus, the error calculated from the experiment data and model prediction is concluded to be following the normal distribution.

Montgomery (2001) stated that if the model is correct and if the assumptions are satisfied, the residual should be structureless, in particular, they should be unrelated to any other variable including the predicted response, and this is clearly observed in

Figure 4.6B. It also indicated that that the error observed was due to random error. Histogram for residuals was also plotted to check the normality assumption, and it showed the residuals closely followed normal distribution as the standardized residual distribution is centered at zero within acceptable range of -2 to 2 (Figure 4.6C).

The standardized residual versus observation order was plotted to check whether the order of the experimental runs affected the collected data. From Figure 4.6D, the random pattern indicated that observation order has no influence on the collected data, and that the error was well distributed within acceptable range of -2 to 2.

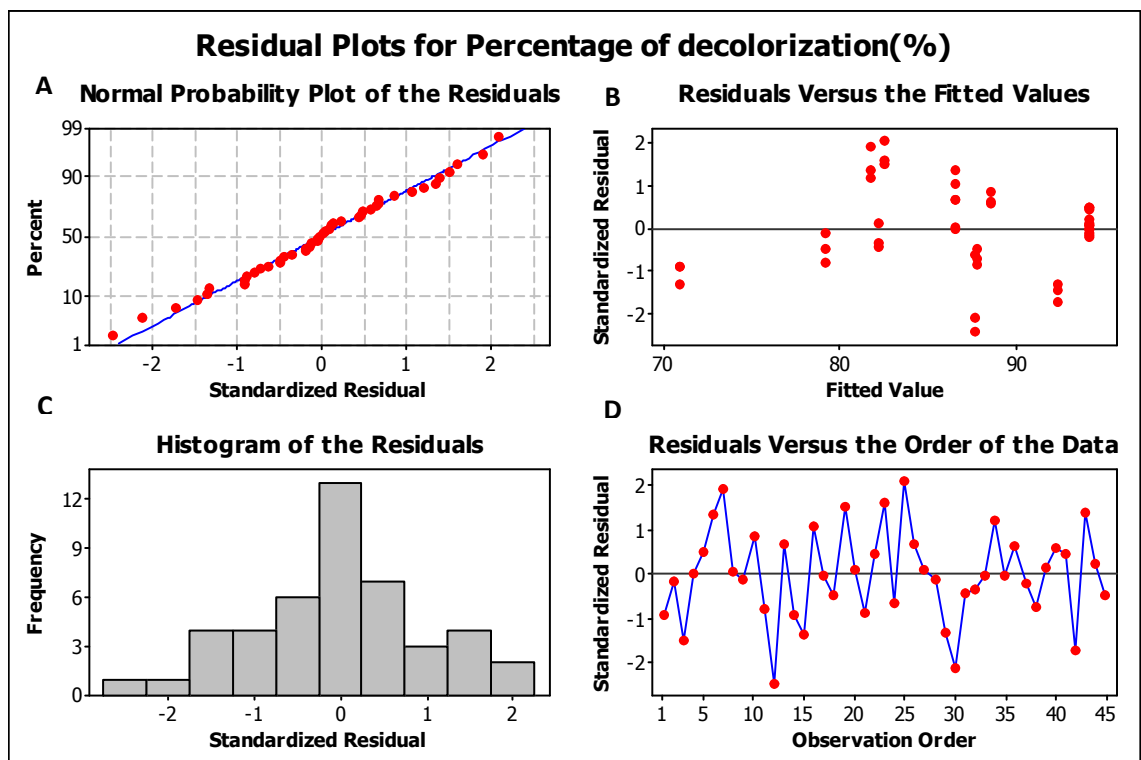


Figure 4.6: Residual plots for percentage of decolorization

Figure 4.7 showed the main effect plot of the data mean for the percentage of the dye decolorization. The steeper the line indicates the stronger effect of the parameter on the response (i.e. dye decolorization). In this experiment, process time (Figure 4.7A)

showed positive gradient initially and shift to negative gradient after 2 days. This indicates that percentage of decolorization increase with longer process time. However, after 2 days, the decolorization was negatively affected. This observation was attributed to the possibilities of other metabolites being produced by *P. sanguineus* which are also able to absorb light within the range of absorption wavelength for the crystal violet.

Agitation speed factor showed the steepest line compared to the other factors (Figure 4.7B). This was interpreted as the factor that has most significant effect on the decolorization process. The decolorization percentage increased when the agitation speed was varied from 60 rpm to 110 rpm. However, it started to reduce at the highest speed studied *i.e.* at 160 rpm. The reason could be due to the fungus beginning to be negatively affected mechanically due to more intense agitation. Initial dye concentration (Figure 4.7C) is influencing the response the weakest among the factors tested. The positive gradient of the graph showed that the higher initial dye concentration, the higher percentage of decolorization was achieved although the differences were relatively small.

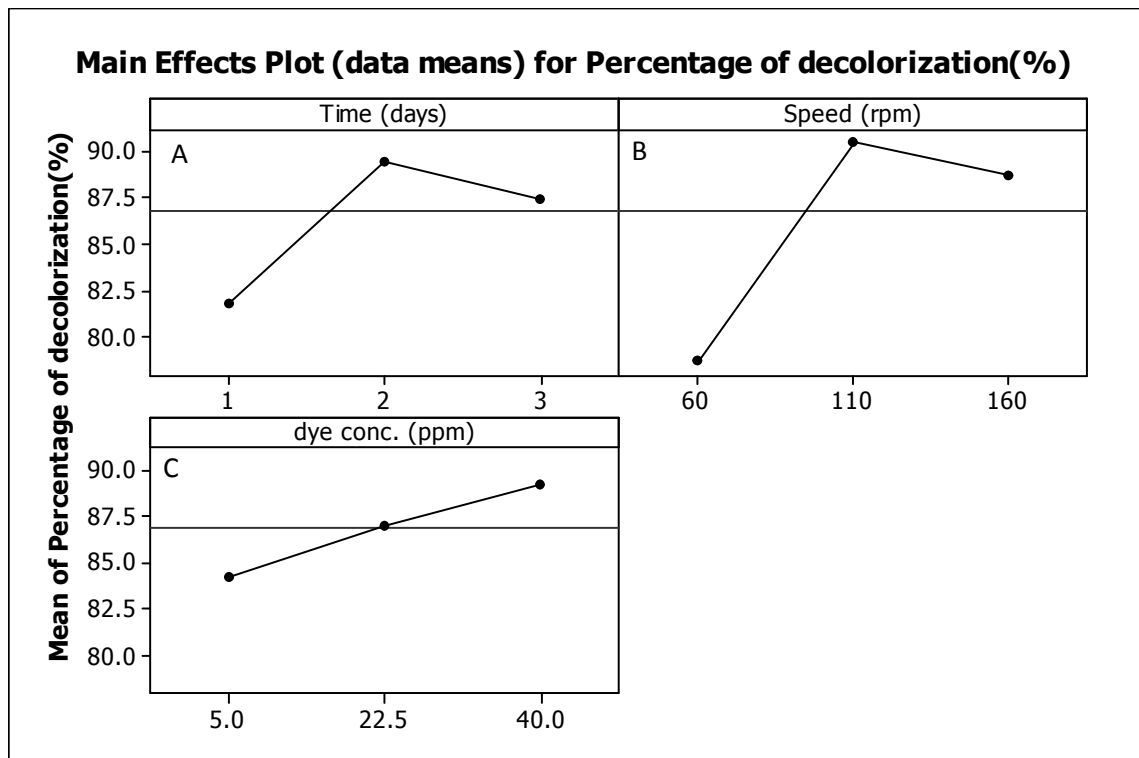


Figure 4.7: Main effects plot (data means) for percentage of decolorization

Figure 4.8 showed an overlaid contour plot for the two interacting variables *viz.* process time and agitation speed. The white region shown is the feasible area for optimization with decolorization percentage at 90 % and above. The highest percentage of decolorization was achieved within this region ( $\geq 90\%$ ) under 90 to 160 rpm of agitation speed and 1.4 to 3.0 days of process time.

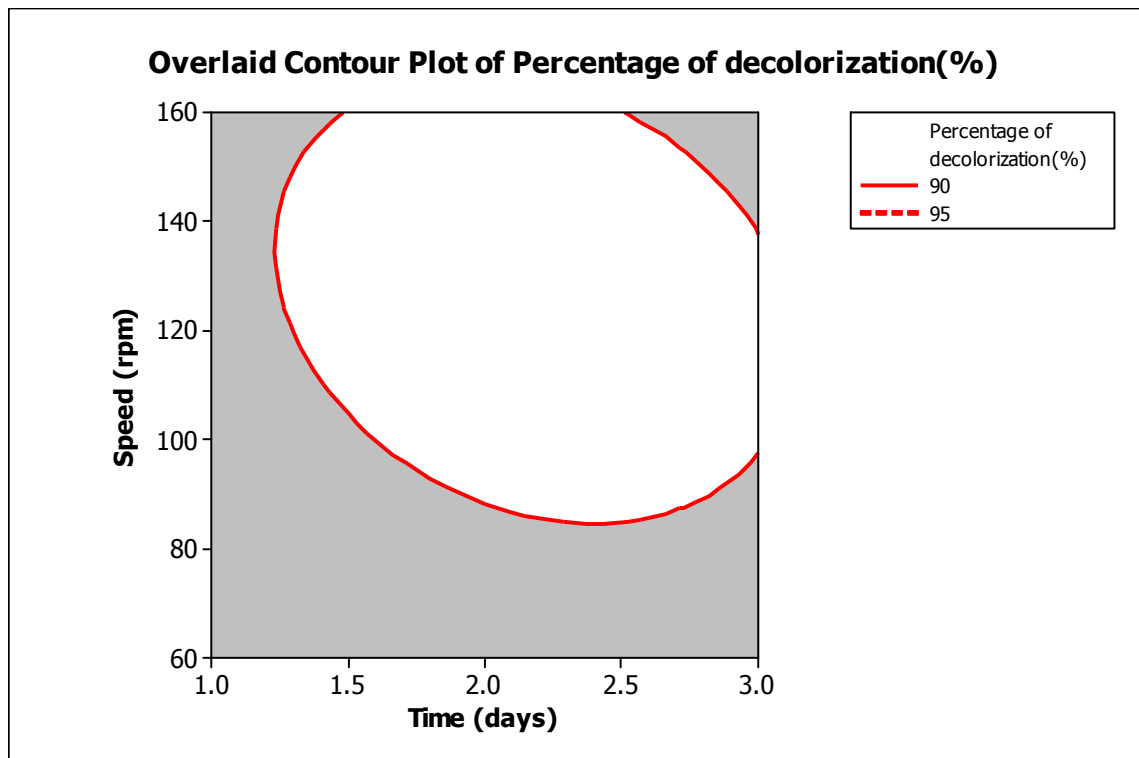


Figure 4.8: Overlaid contour plot

Figure 4.9 showed contour plot for process time and agitation speed. Lower percentage of decolorization occurred at lower agitation speed with lower process time of decolorization. At lowest agitation speed (60 rpm), dye decolorization increase up to 80 to 85% after 3 days process time. At lowest process time for decolorization, percentage of decolorization also increased up to 85 to 90 % within 110 to 160 rpm. The maximal decolorization process was observed at darkest region where the combination involving occurred at higher agitation speed (about 90 rpm to 160 rpm) with longer process time (about 2 to 3 days).

However, there is a small region at highest speed (approximately 140 rpm to 160 rpm) with longest decolorization time (approximately 3 days) where the percentage of decolorization reduced from the range of 95 % and above to 85 % to 90 %. It may be due to stress condition experienced by when fungus exposed to more intense agitation

environment. Longer process time also exposed the fungus to longer duration of starvation condition inside the dye solution which contains no available nutrients. Furthermore, Rajesh and Uttam (1999) stated that this triphenylmethane is an effective chemical for controlling fungal growth. However, the concentration level that is effective in controlling the fungal growth depends on the fungal strains and exposure conditions. Thus, crystal violet may also exert its toxicity towards *P. sanguineus*.

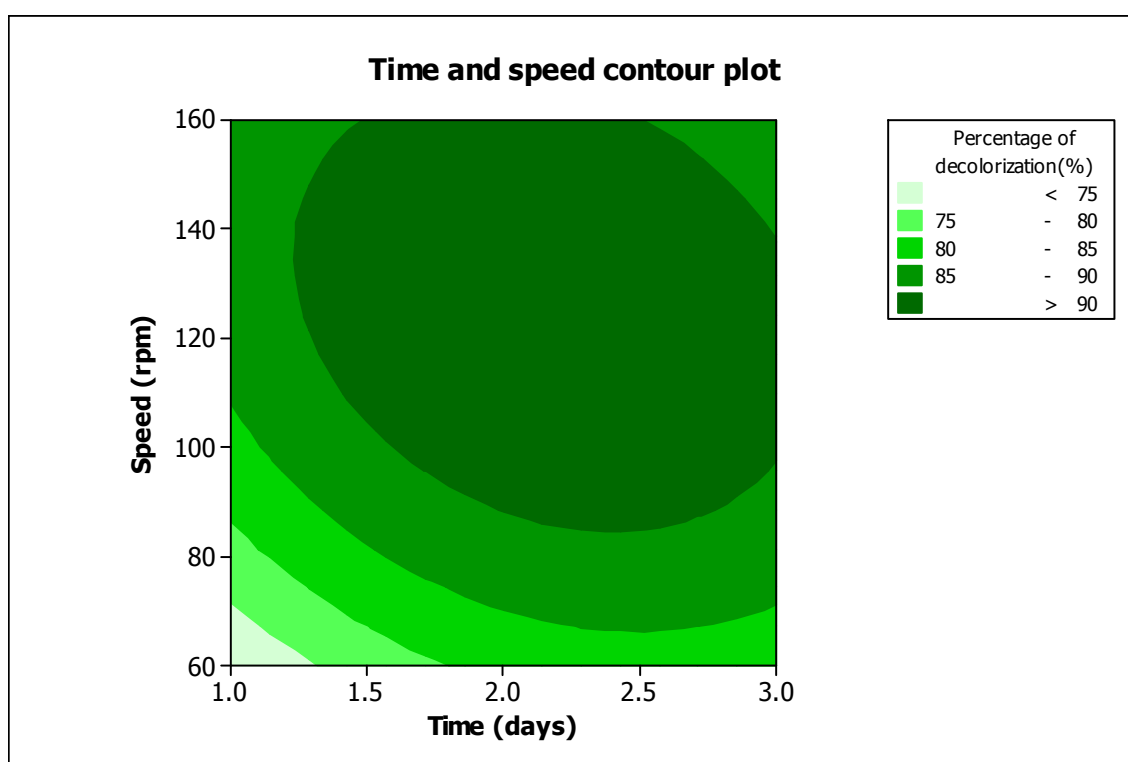


Figure 4.9: Process time and agitation speed contour plot

Based on these analyses, optimization was performed using Response optimizer function of MINITAB<sup>®</sup> 14 software. The starting condition for optimization were 40 ppm of initial dye concentration, 2 days of process time and 110 rpm of agitation speed. The goal for optimization was maximize the decolorization process. The local and global solutions returned by optimization routine were 2 days process time and 128 rpm



of agitation speed respectively with desirability and composite desirability of 0.98 respectively. Thus, it is predicted that under the optimal conditions, it is possible to achieved 94.4 % decolorization.

To validate the predicted optimum values for the studied variables, additional experiments were conducted under the predicted condition. Independent experiments were performed at 2 days process time, 128 rpm agitation speed and 40 ppm initial dye concentration. The average decolorization percentage obtained was  $95.0 \pm 0.3$  %. Since the average value ( $95.0 \pm 0.3$  %) was higher than the predicted value (94.4 %), further *t*-test was done ( $p > 0.05$ ) to show that there was no significant difference between the mean of measured values and the predicted value for dye decolorization under optimal conditions.

#### **4.4 Control experiment**

The dye degradation was ascribed to laccase activity as this is the sole phenoloxidase that is produced by *P. sanguineus* in submerged culture (Pointing *et al.*, 2000). However, colored pellets was observed after decolorization process indicate that decolorization of the dye solution could have also occurred by adsorption. Control experiment was carried out to find out the extent of adsorption of the dye by heat killed *P. sanguineus* pellets. Under optimal condition, it was found that as much as  $45.2 \pm 4.2$  % decolorization was achieved *via.* physical adsorption of the dye to fungal biomass (pellets). This indicated that probably only approximately 48 % of crystal violet decolorization could be attributed to laccase activity whereas the remainder was due to adsorption by fungal pellets.

## 4.5 Stirred tank reactor (STR)

Observation on the flow of liquid for dye decolorization process showed different pattern between the experiments ran using angled blade  $60^\circ$  and curved blade impeller. For angled blade  $60^\circ$  impeller, the liquid streaming downwards from the impeller deviates from its vertical (axial) direction to the horizontal direction. Then, the liquid flows horizontally along the bottom and changing the direction from the bottom upwards (vertically) along the wall of the cylindrical vessel when the volumetric flow rates of the liquid taking place in the downward and upward flows are same (Figure 4.10A). Curved blade impeller showed the radial-flow impeller pattern (Figure 4.10B). When the stirrer is set up by rotation, the liquid is driven radially from the impeller against the walls of the tank. It then divides into two streams, one flowing up to the top of the tank and the other flowing down to the bottom.

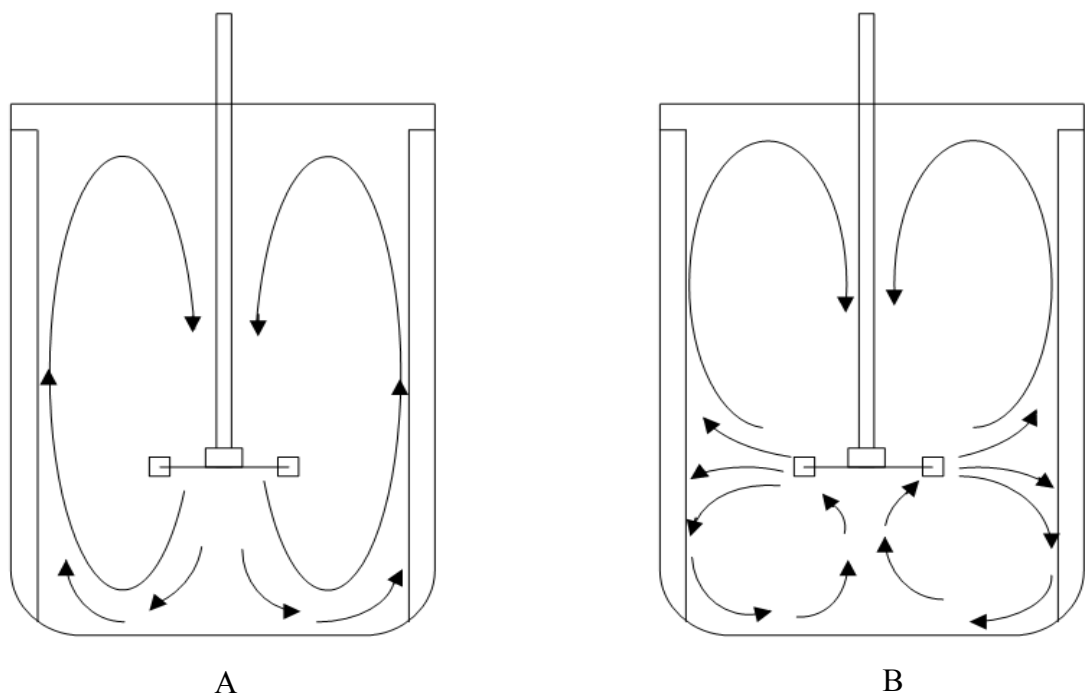


Figure 4.10: Flow pattern of different impeller, A: angled blade  $60^\circ$  impeller, B: curved blade impeller

The time profile of crystal violet decolorization by *P.sanguineus* in STR using curved blade impeller at different speeds is shown in the Figure 4.11. Decolorization occurred significantly after first 12 hours, where decolorization achieved was approximately  $81.4 \pm 0.3$  % (for 60 rpm of speed) to  $83.9 \pm 0.5$  % (for 120 rpm of speed). From 12 hours to 60 hours, percentage of decolorization did not increase further. The highest decolorization was  $90.6 \pm 0.01$  % achieved at 120 rpm after 60 hours decolorization time.

When angle blade  $60^\circ$  impeller was used, it showed significant decolorization after 12 hours within the range of  $75 \pm 0.2$  % (for 120 rpm of speed) to  $87.9 \pm 0.1$  % (60 rpm of speed) (Figure 4.12). For the first 24 hours, the results showed that the higher the speed, the lower percentage of decolorization. However, after 12 hours, there was no further decolorization pattern observed. The highest decolorization was  $92.9 \pm 0.02$  % at 60 rpm after 60 hours decolorization time.

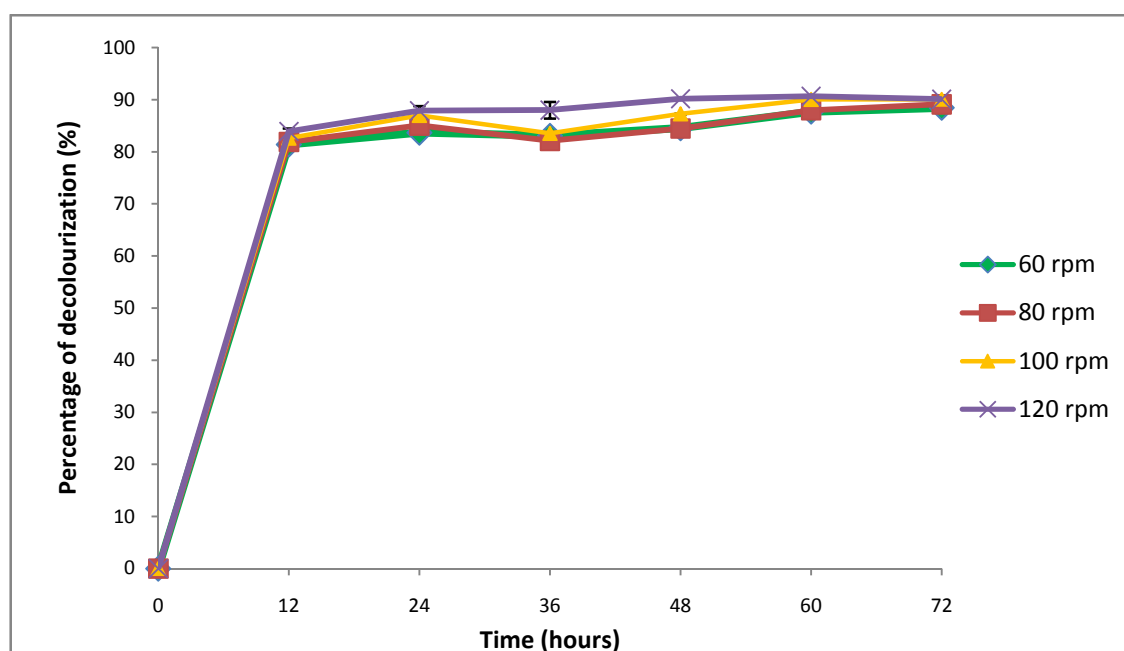


Figure 4.11: Crystal violet decolorization by *P. sanguineus* using curved blade impeller

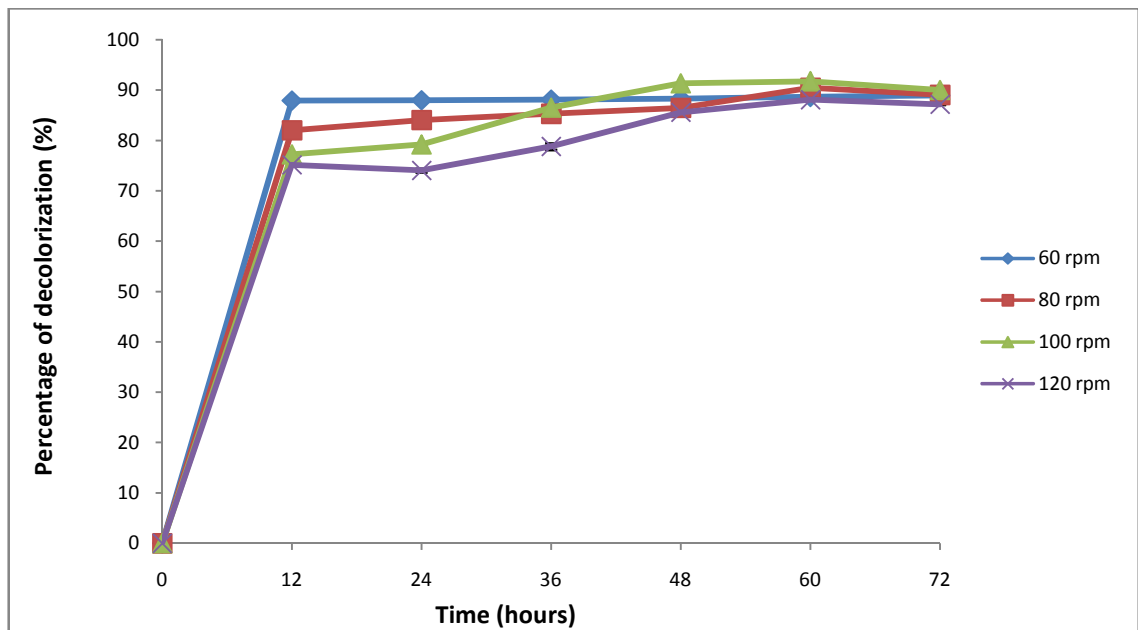


Figure 4.12: Crystal violet decolorization by *P. sanguineus* in stirred tank reactor using angled blade 60°

Figure 4.13 shows the effect of speed on the decolorization process using curved blade and angled blade 60° impeller. Generally, curved blade and angled blade 60° had showed different pattern against percentage of decolorization at varying impeller speed. Curved blade impeller showed that the higher the speed, the higher percentage of decolorization whereas angle blade 60° impeller showed that the percentage of decolorization decreased by increase the impeller speed. However, angled blade 60° impeller had more pronounced effect on decolorization process at varying impeller speed *i.e.* 60 to 120 rpm as it has steeper line compared to the curved blade impeller (Figure 4.13).

For 12 hours process time (Figure 4.13A), the experiment using curved blade impeller showed the percentage of decolorization was increased from  $82.3 \pm 0.04$  % to  $84.0 \pm 0.9$  % by increase the impeller speed from 60 to 120 rpm. However, experiment on angled blade 60° showed that percentage of decolorization decrease from  $87.9 \pm 0.05$  % to  $75.2 \pm 0.4$  % by increase the speed from 60 to 120 rpm.

At 24 hours decolorization time (Figure 4.13B), percentage of decolorization for the curved blade also increase by increase the impeller speed from  $83.7 \pm 0.12$  % (60 rpm) to  $87.7 \pm 0.9$  % (120 rpm) while angled blade impeller showed that the percentage of decolorization decrease from  $8.3 \pm 0.06$  % to  $74.1 \pm 0.6$  % with increasing the speed from 60 to 120 rpm.

There was no significant effect on percentage of decolorization observed at varying speed of impeller after 24 hours process time for both curved blade and angle blade  $60^\circ$  impeller (Figure 4.13C,D,E,F). This explained that after 24 hours, any changes in percentage of decolorization could be related to the fungus itself, and not necessarily the different impellers' geometries. After 24 hours, the fungus was in starvation condition where there was no nutrient inside the dye solution consequently reducing their productivity of laccase *viz.* catalyst for decolorization process.

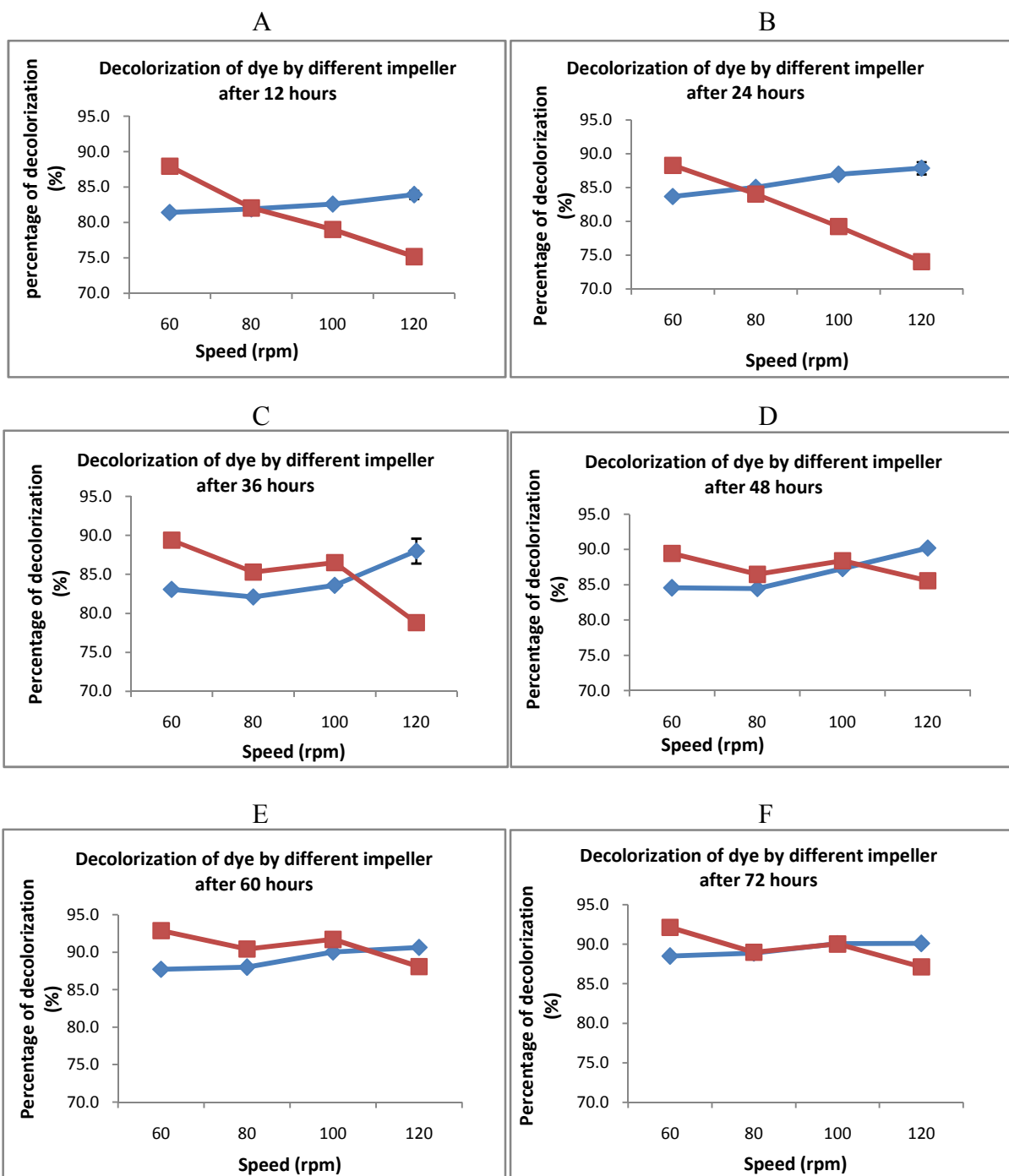


Figure 4.13: Plot of percentage of decolorization (%) versus agitation speed (rpm) for decolorization of crystal violet by *P. sanguineus* using curved blade impeller (—◆—) and angled blade 60° (—■—) in a stirred tank reactor. The figures (A-F) represented reading from 12 hours to 72 hours respectively where A=12 hours, B=24 hours, C=36 hours, D=48 hours, E=60 hours and F=72 hours

Table 4.7 showed the calculated power consumption at varying speed for curve blade impeller and angle blade 60° impeller. Based on the pattern of decolorization studied, angle blade 60° is the better impeller for decolorization as compared to curved blade impeller as better decolorization was achieved at lower speed consequently reducing the power consumption for the process in the long run.

Table 4.7: Values of power consumption at varying speed for curved blade impeller and angled blade 60°

Speed of impeller (rpm)	Power ( $P=N_p\rho N^3 D^5$ )(kW)	
	Curved blade impeller	Angled blade 60° impeller
60	3301	3689
80	7824	8745
100	15281	17079
120	26406	29513